UCRL- 91476
PREPRINT
CONF - 840963--2

OPTICAL GUIDING BY A FREE ELECTRON LASER

E. T. Scharlemann
A. M. Sessler
J. S. Wurtele

MASTER

This paper was prepared for submittal to
Workshop on Coherent/Collective Propagation of Relativistic
Electron-Beams/Electromagnetic Radiation
Villa Olmo, Como, Italy
September 13-16, 1984

October 16, 1984

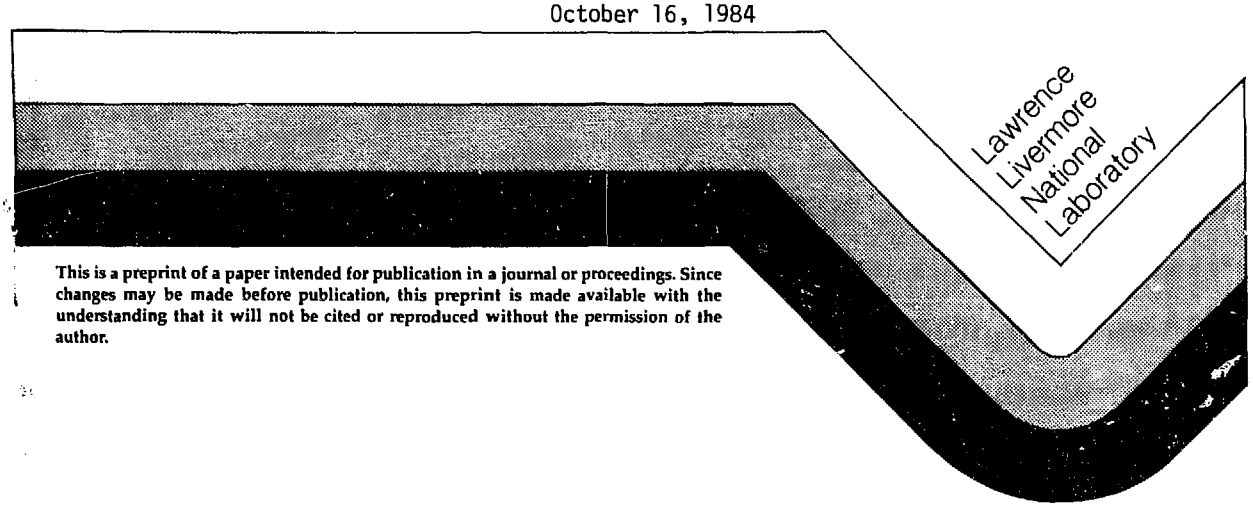

OPTICAL GUIDING IN A FREE ELECTRON LASER

E. T. Scharlemann
University of California
Lawrence Livermore National Laboratory*
Post Office Box 808/L-321
Livermore, CA 94550

A. M. Sessler and J. S. Wurtele**
Lawrence Berkeley Laboratory+
One Cyclotron Road/58-101
Berkeley, CA 94720

UCRL--91476

DE85 003141

October 16, 1984

ABSTRACT

The coherent interaction between an optical wave and an electron beam in a free electron laser (FEL) is shown to be capable of optically guiding the light. The effect is analyzed using a two-dimensional approximation for the FEL equations, and using the properties of optical fibers. Results of two-dimensional (cylindrically symmetric) numerical simulations are presented, and found to agree reasonably well with the analytically derived criterion for guiding. Under proper conditions, the effect can be large and has important applications to short wavelength FEL's and to directing intense light.

* Work performed jointly under the auspices of the U. S. Department of Energy by Lawrence Livermore National Laboratory under contract W-7405-ENG-48 and for the Department of Defense under Defense Advanced Research Projects Agency ARPA Order No. 4395 Amendment No. 31, monitored by Naval Surface Weapons Center under document number N60921-84-WR-W0080.

+ This work was supported by the Director, Advanced Energy Systems, Basic Energy Sciences, Office of Energy Research, US DOE under contract number DE-AC03-76SF00098.

** Present Address: Plasma Fusion Center, Massachusetts Institute of Technology

I. INTRODUCTION

It has long been known that the coherent interaction between the light and the electron beam in an FEL produces a phase shift of the light [1], and that the sign of the effect is such that the light is refracted toward the electron beam [1,2]. In recent numerical simulations we have observed guiding of the light by the electron beam, as if the electron beam were an optical fiber [3,4]. These observations stimulated the investigation reported on here.

In this work we treat the bunched electron beam as if it were an optical fiber with a constant index of refraction and a well-defined edge. In Sec. II we review the properties of such step-profile optical fibers for a real or complex index of refraction. In Sec. III, we use one-dimensional FEL theory to evaluate the index of refraction of the electron beam, and present numerical simulations to illustrate optical guiding. We then examine, in Sec. IV, guiding in the exponential growth regime. We find that the intuitive criterion for guiding during exponential growth,

$$\alpha z_r > 1 \quad , \tag{1.1}$$

can be strongly violated. Here the field amplitude grows as $e^{\alpha z}$, and z_r is the Rayleigh length obtained from the electron beam size and light wavelength. The analytical derivations are compared with the results of numerical simulations. Finally, in Sec. V, we mention several potential applications of self-guiding.

II. OPTICAL PROPAGATION IN FIBERS

In this section, we review the salient facts about circular step-profile optical fibers, with emphasis on the LP_{01} mode, the lowest order, linearly polarized mode. This is the mode that the numerical calculations model, and which one would expect to be excited in an FEL with a linear wiggler. We determine the value of the fiber parameter (defined below) necessary for optical guiding.

The usual analysis of step profile fibers [3,4] assumes that the fiber consists of a central core of radius a and index of refraction n, and a cladding of index n_{cl}. In our treatment, the core is the electron beam and the cladding is free space.

We can make the assumption that the fiber is weakly guiding:

$$|n - 1| \ll 1 \quad . \tag{2.1}$$

This inequality is quite good for all cases of interest, and is consistent with the assumption of slowly varying phase of the optical field:

$$\frac{d\phi}{dz} \ll k \quad , \tag{2.2}$$

familiar from FEL theory

Following Marcuse [4], we consider guided modes with only one transverse electric field component E_x (but both magnetic and electric longitudinal components), for which

$$E_x = AJ_\nu(\kappa r) \begin{pmatrix} \cos(\nu\phi) \\ \sin(\nu\phi) \end{pmatrix}, \; r < a \quad , \tag{2.3}$$

$$E_x = A \frac{J_\nu(\kappa a)}{H_\nu^1(i\gamma a)} H_\nu^1(i\gamma r) \begin{pmatrix} \cos(\nu\phi) \\ \sin(\nu\phi) \end{pmatrix}, \quad r > a \quad . \tag{2.4}$$

In Eq. (2.3) and (2.4), J_ν and H_ν^1 are Bessel functions and Hankel functions of the first kind, respectively. The arguments of the functions are

$$\kappa = \sqrt{n^2k^2 - \beta^2} \quad , \tag{2.5}$$

$$\gamma = \sqrt{\beta^2 - k^2} \quad , \tag{2.6}$$

$$k = \frac{\omega}{c} \quad , \tag{2.7}$$

and the field is assumed to vary as

$$e^{i(\beta z - \omega t)} \quad . \tag{2.8}$$

Continuity of B_z and E_z at the fiber edge yields the dispersion relation:

$$\frac{\kappa J_{\nu+1}(\kappa a)}{J_\nu(\kappa a)} = \frac{\gamma K_{\nu+1}(\gamma a)}{K_\nu(\gamma a)} \tag{2.9}$$

with

$$(\kappa^2 + \gamma^2)\, a^2 \equiv V^2 = (n^2 - 1)\, k^2 a^2 \quad . \tag{2.10}$$

The quantity V is called the "fiber parameter".

The condition for mode cutoff in a fiber is

$$\gamma a \to 0 \quad . \tag{2.11}$$

In this limit the dispersion relation, Eq. (2.9), simplifies to

$$J_1(V_c) = 0 \quad \text{if } \nu = 0 \quad , \tag{2.12}$$

and

$$J_0(V_c) = 0 \quad \text{if } \nu = 1 \quad . \tag{2.13}$$

In Eq. (2.12) V_c is the value, at cutoff, of the fiber parameter V. Clearly, since increasing V means more zeros of the Bessel functions which satisfy $V_c < V$, the fiber parameter measures the number of guided modes supported by the fiber. Note that from Eq. (2.12) there is no cutoff for the LP_{01} mode. (The first index labels the Bessel function, the second labels the zero's.)

While formally there is no cutoff for the LP_{01} mode, it is incorrect to think of the mode as bound by the fiber for all $V > 0$. To examine this more closely, near cutoff ($\gamma a \ll 1$) the $\nu = 0$ modes satisfy:

$$\gamma a = 1.12 \exp\left(-\frac{J_0(V)}{V\, J_1(V)}\right) \quad . \tag{2.14}$$

Since the mode amplitude falls off radially as $\exp(-\gamma r)$ for large γr, $1/\gamma$ measures the radial extent of the mode. An examination of Eq. (2.14) shows the mode extends far outside the beam for $V \ll 1$.

For the LP_{01} mode to be considered guided, we will somewhat arbitrarily require that the 1/e point of E_x be within 5 times the fiber radius. This condition corresponds to demanding that

$$V^2 > 1 \quad . \tag{2.15}$$

The analysis can be extended to a fiber with gain (or loss) by permitting V to be complex. The dispersion relation, Eq. (2.9), is unchanged, but κ and γ can now also be complex. From numerical solution of the complex dispersion relation, we find the above criterion (2.15) generalizes to

$$\mathrm{Re}(V^2) + 1/2\ \mathrm{Im}(V^2) > 1 \quad . \tag{2.16}$$

The nature of the solution, however, is different -- a complex γ corresponds to propagation of radiation away from the fiber, balanced by gain in the fiber.

If we examine light propagation in an infinite parabolic medium with gain [5] we obtain an analogous criterion for guiding.

III. THE INDEX OF REFRACTION OF AN ELECTRON BEAM

3.1 General Analysis

The electron beam in a high-gain FEL physically bunches on an optical wavelength; because of the bunching, the beam has an effective index of refraction greater than unity. This is in sharp contrast to the behavior of an unmagnetized (and unbunched) plasma, and is the basis for the optical guiding effects described in this paper. In the previous section, we have presented the criterion that the index of refraction must satisfy in order for a fiber to guide the laser beam; in this section we derive the index of refraction of an electron beam in an FEL.

As a further preliminary, we wish to draw a distinction between two effects, which we will label "refractive guiding" and "gain focusing". The first refers to the familiar guiding of an optical beam by a fiber with a real index of refraction. The power in the optical beam propagates exactly parallel to the fiber. The second, gain focusing, refers to self-similar propagation of an optical beam profile around a fiber with gain: power diffracts away from the fiber, but the gain in the fiber more than balances diffraction. The result is an optical

profile that grows in amplitude, but does not change shape (hence the description as self-similar propagation). The distinction between these two cases is primarily in the nature of the index of refraction. Gain focusing occurs around a fiber with a purely imaginary index of refraction; refractive guiding when the index of refraction is purely real. In an FEL, the effective index of refraction is complex, producing a mixture of refractive guiding and gain focusing; in the examples we present, refractive guiding dominates.

Refractive guiding alone dominates in at least two circumstances: a) after saturation in an untapered wiggler (when the light intensity is roughly constant), and b) in a tapered wiggler. The real part of the index of refraction of an optically bunched beam comes from the FEL equations as formulated in Ref. 6:

$$\mathrm{Re}(n)-1 \equiv \frac{1}{k}\frac{d\phi}{dz} = \frac{2\pi e J\, a_w}{mc^3 k e_s} \left\langle \frac{\cos\psi}{\gamma} \right\rangle \quad . \tag{3.1}$$

Gain focusing may dominate in the exponential gain regime of an FEL with an untapered wiggler. The general expression for the imaginary part of the index of refraction comes from the amplitude equation:

$$\mathrm{Im}(n) \equiv \frac{1}{k e_s}\frac{de_s}{dz} = \frac{2\pi e J\, a_w}{mc^3 k e_s} \left\langle \frac{\sin\psi}{\gamma} \right\rangle \quad . \tag{3.2}$$

In Eq. (3.1) and (3.2), e_s is the normalized r.m.s amplitude of the electric field:

$$e_s \equiv \frac{e\,|E_s|}{\sqrt{2}\,mc^2} \tag{3.3}$$

(for a linear wiggler); a_w is the dimensionless r.m.s. vector potential of the wiggler field:

$$a_w \equiv \frac{e\,|B_w|}{\sqrt{2}\,k_w\,mc^2} \tag{3.4}$$

where k_w is the wiggler wavenumber. The current density is J, ψ is the phase of an electron in the pondermotive potential well, and the brackets denote an average over the electron distribution. We use Gaussian c.g.s. units.

From Eq. (3.1) and (3.2) we see that refractive guiding and gain-focusing are distinguished simply by whether $<\frac{\cos\psi}{\gamma}>$ or $<\frac{\sin\psi}{\gamma}>$ dominates; i.e., by the relative phase between the electron bunches and the laser electric field.

The expressions for n in Eq. (3.1) and (3.2) are derived for a uniform infinite medium and a plane electromagnetic wave. We use the value of the index on the electron beam axis to determine the fiber parameter V. The relationships among $d\phi/dz$, de_s/dz and n are changed by two-dimensional effects, as described in Sec. IV.

3.2 Examples of FEL Guiding

In this section, we present numerical simulations to illustrate guiding in the exponential gain regime (which we discuss in detail in Sec. IV), and guiding in an untapered wiggler after saturation. The

simulations were performed at LLNL with the 2-dimensional FEL code FRED. An earlier version of the code is described in Ref. [7] and [8]; the code has since been modified to include full betatron motion of the electrons. The code follows an axisymmetric laser beam around an electron beam that bunches longitudinally (in ψ [1]). Axisymmetric diffraction effects are fully included, via the paraxial wave approximation; refractive and gain effects are included through the local source terms provided by the electron beam.

The two categories of FEL guiding can be illustrated with a single simulation, based on the design of an FEL in a storage ring. The parameters of the simulation are listed in Table I. Figure 1 is a three-dimensional contour plot of laser intensity versus r and z. The initial bump in the laser intensity on axis is the input 30 MW laser beam at a focus; guiding is evident in the later growth of the laser field, and in the saturated regime (past 16 m). The guiding is visible more quantitatively in Figs. 2 through 4, which are cross-sections of the laser profile at several values of z. The laser profile is nearly constant over 60 Rayleigh lengths of propagation. Figure 2 is a cross-section in the exponential gain regime, Fig. 3 in the saturated regime, and Fig. 4 at the end of the wiggler. An interesting effect of the guiding is illustrated in Fig. 5, which is a plot of the phase of the electric field versus radius at the end of the wiggler: the decrease in ϕ with increasing r indicates that the output laser beam is actually converging to a focus 8 cm beyond the end of the wiggler.

3.3 Guiding After Saturation

After saturation, the guiding of the light is entirely refractive, and Eq. (3.1) is applicable. We can generally take the bunching term, $\langle(\cos\psi)/\gamma\rangle$, to be $\simeq 1/2\gamma_0$, where γ_0 is the average electron Lorentz factor. $\cos\psi$ must of course remain less than or equal to unity, and perfect bunching at $\psi=0$ never occurs. Then, for the parameters of the simulation, we find

$$\mathrm{Re}(V) \simeq 1 \quad , \tag{3.5}$$

after saturation.

For guiding of the light after saturation, we obtain in general

$$V^2 \simeq \frac{2eI}{mc^3}\,\frac{ka_w}{\gamma_0 e_s} \gtrsim 1 \quad , \tag{3.6}$$

where I is the total current. With a slight modification, this equation is applicable to tapered wiggler amplifiers; the expression for V^2 must be multiplied by $\simeq 2f_{\mathrm{trapped}}\cos\psi_r$, where f_{trapped} is the fraction of the electrons trapped in the decelerating ponderomotive potential well [1], and ψ_r is the resonant ψ of an electron that decelerates with the bucket.

IV. GUIDING IN THE EXPONENTIAL GAIN REGIME

We can analyze the guiding in the exponential gain regime by extending the linear analysis in Ref. [9] to include the effects of diffraction (and incidentally, energy spread). To do so, we write the longitudinal

electron equations derived by Kroll, Morton, and Rosenbluth [1] in complex form:

$$\frac{d\gamma_j}{dz} = \mathrm{Re}\left[i \frac{a_w f_B}{\gamma_j} e_s e^{i\theta_j} \right] , \tag{4.1}$$

$$\frac{d\theta_j}{dz} = \mathrm{Re}\left[k_w - \frac{k}{2\gamma_j^2} (1 + a_w^2) - \frac{a_w f_B e_s}{\gamma_j^2} e^{i\theta_j} \right] . \tag{4.2}$$

In Eq. (4.1) and (4.2), θ_j is the phase of an electron with respect to a plane wave; in terms of ψ_j and ϕ,

$$\theta_j \equiv \psi_j - \phi . \tag{4.3}$$

The factor f_B is the well-known difference of Bessel functions [10].

The complex field equation follows from Eq. (3.1) and (3.2), but with addition of a transverse gradient term:

$$\frac{\partial e_s}{\partial z} = \frac{2\pi i e\, a_w}{mc^3} f_B \frac{J}{N} \sum_j \frac{e^{i\theta_j}}{\gamma_j} + \frac{i \nabla_\perp^2 e_s}{2k} , \tag{4.4}$$

where e_s is now a complex field amplitude. The total number of electrons is N. The transverse gradient term follows directly from the paraxial wave equation [11]. The recognition that a guided laser field propagates with an unchanged profile permits us to approximate the transverse gradient term very simply:

$$\frac{\nabla_\perp^2 e_s}{2k} \simeq - \frac{e_s}{z_r} \tag{4.5}$$

where $z_r \equiv kw^2/2$ for a Gaussian profile with an electric field 1/e radius of w. The self-similar profile of a guided beam is not Gaussian; hence the approximate nature of Eq. (4.5).

Equations (4.1), (4.2), and (4.4) can now all be linearized, taking e_s to vary as $e^{i\lambda(z/zr)}$. To incorporate an electron energy spread, we take a square distribution for the electron energy:

$$f(\gamma) = \frac{1}{2\Delta\gamma} , \quad \gamma_0 - \Delta\gamma \leq \gamma \leq \gamma_0 + \Delta\gamma$$
$$= 0 , \quad \text{otherwise.} \tag{4.6}$$

The result of linearization is a cubic in the complex, dimensionless parameter λ:

$$\lambda^3 + \lambda^2 [1 + 2\,\Delta k_0\, z_r]$$
$$+ \lambda \left[2\,\Delta k_0\, z_r + (\Delta k_0 z_r)^2 - 4(k_w z_r)^2 \frac{\Delta\gamma^2}{\gamma_0^2} \right] \tag{4.7}$$
$$+ A\, k_w z_r + (\Delta k_0 z_r)^2 - 4(k_w z_r)^2 \frac{\Delta\gamma^2}{\gamma_0^2} = 0 .$$

Here

$$\Delta k_0 \equiv k_w - \frac{k}{2\gamma_0^2} (1 + a_w^2) \tag{4.8}$$

is a parameter that measures the departure from resonance of the center, γ_0, of the electron distribution function, and

$$A \equiv \frac{4\pi e J}{mc^3} \frac{a_w^2 f_B^2}{\gamma_0^3} z_r^2 \tag{4.9}$$

is the dimensionless parameter that measures the coupling between the electron beam and the light.

One's natural inclination is to attempt a simplification of this cubic, identifying the dominant terms and discarding the rest. Unfortunately, for many applications, all terms in the cubic are comparable, and the standard general expression for the analytic solution to a cubic must be used.

The expression for the fiber parameter V of the electron beam in terms of λ is simple, and comes from Eqs. (3.1), (3.2), (4.4) and (4.5):

$$V^2 = \frac{2ka^2}{z_r} (1 + \lambda) \quad . \tag{4.10}$$

We take the 1/e point of the Gaussian transverse density profile of the electron beam to be an effective fiber radius. For the parameters of the simulation described in Section 3.3, with w=0.02 cm (as observed in the simulation), the cubic yields

$$\begin{aligned} V^2 &= 1.03 - 0.12i \\ \lambda &= 0.03 - 0.12i \end{aligned} \tag{4.11}$$

Our criterion for guiding [Eq. (2.16)] is satisfied, although the laser beam is somewhat more tightly confined to the electron beam than $|V| = 1$ would predict. In terms of either the assumed w, or V, the discrepancy is only about 20 percent.

The value for $|\mathrm{Im}(\lambda)|$ is consistent with the exponential gain observed in the simulation. The fact that $\mathrm{Im}(\lambda)$ is much less than unity indicates that the gain length is much longer than the Rayleigh range,

strongly violating the naive criterion mentioned in the Introduction, Eq. (1.1).

The general procedure for evaluating the importance of guiding laser light by an electron beam is iterative. The cubic, Eq. (4.7), is solved with an assumed value for w; twice the electron beam radius (w=2a) is a good initial guess. From the solution for λ, Eq. (4.10) gives V. The value of V determines, through Eq. (2.9) and (2.10), values for γ and . The quantity w is then given by

$$w \simeq 1/\ |\mathrm{Re}(\gamma)| \quad . \tag{4.12}$$

Iterating produces a consistent solution for the laser beam size and the growth rate, if a guided solution exists.

We have assumed that the transverse derivative term in Eq. (4.5) can be adequately approximated by using w, the light beam size -- this assumption permitted us to use the Rayleigh range of the laser profile in the derivation. When $w \gg a$, or $V^2 < 1$, this assumption is violated; for $V^2 < 1$, the transverse derivative term must be written as

$$\nabla_\perp^2 e_s = - \kappa^2 e_s \tag{4.12}$$

with κ obtained from the fiber dispersion relation. An interesting example of this limit occurs when the electron beam current becomes very small ($A \to 0$), with $\Delta k_0 = \Delta\gamma = 0$. Then the cubic Eq. (4.7) reduces to

$$\lambda^3 + \lambda^2 + A\, k_w z_r = 0. \tag{4.13}$$

Perturbing around the roots $\lambda = 0, 0, -1$ obtained with $A = 0$, we find

$$\lambda = \pm i \sqrt{A k_w z_r}, \quad - A k_w z_r \quad . \tag{4.14}$$

All three roots correspond to $V^2 \ll 1$ and $w \gg a$, as one would expect.

The growing root in Eq. (4.13), $\lambda = - i \sqrt{A k_w z_r}$, is very different from what one would expect from one-dimensional theory, with or without a fill factor. The growth rate is less, and scales as $J^{1/2}$ rather than $J^{1/3}$; the physical reason for the difference is the importance of diffraction in this limit.

As one would expect, diffraction decreases the linear growth rate. The effect of diffraction on guiding is unexpected, however, and can be seen from the form of Eq. (3.1) and (3.2). For a given bunching $\langle(\cos\psi)/\gamma\rangle$, diffraction reduces the electric field e_s. The index of refraction of the electron beam is thereby increased, enhancing the guiding. It is this enhancement that permits exponential gain even when Eq. (1.1) is violated.

V. APPLICATIONS

We have been motivated in this study, and have emphasized in this paper, the importance of optical guiding (under some circumstances) to FEL performance. As we have seen, the phenomena can be rather important and thus one can contemplate FEL's of exceedingly long length. In this way, it appears possible to have a small electron beam radius and a very long wiggler (hence a very high gain FEL) even in the VUV range.

Because of the effect of optical guiding it is possible to direct and focus the FEL-generated-optical beam. This is of interest for very intense beams, such as are contemplated for laser inertial fusion, where lenses and mirrors of conventional materials would be destroyed by the light. Use of optical guiding appears to be relatively straightforward since a simple magnetic deflection of the electron beam will result in a deflection of the light.

It should be noted that optical guiding applies, also, to very short wavelength light, which does not interact coherently with normal material. Application of this to the VUV and to soft X-rays would appear to make possible some interesting devices.

Optical guiding will be effective in an Inverse Free Electron Laser (IFEL) as well as in an FEL (A. Gaupp, private communication) and hence can be important in the operation of an IFEL, but this requires a large accelerated current.

Finally, we note that optical guiding may make possible resonant ring FEL's (J. D. Dawson, private communication). This requires FEL operation when the FEL is no longer straight, which can be achieved with an isochronous ring. It appears possible, in principle, to have an FEL whose gain is modest per unit length, but whose action extends over many circuits of the ring.

After the completion of this work our attention was drawn to work by G. T. Moore which nicely compliments that presented here [12].

Acknowledgements

We are happy to acknowledge useful conversations with W. M. Fawley, K-J Kim, G. Moore, D. Prosnitz and participants at The Workshop on Plasmas, Accelerators, and Free Electron Lasers at the Aspen Center for Physics, 1984, in particular J. M. Dawson, G. Schmidt, and C-M Tang. We also thank the Aspen Center for Physics where part of this work took place.

Table I

Simulation Parameters

Current (I)	270 A
Electron beam radius in the wiggler (a)	0.01 cm
Electron Lorentz factor (γ_0)	2000
Fractional electron energy spread (r.m.s. $\frac{\Delta\gamma}{\gamma}$)	$1.2 \cdot 10^{-3}$
Laser wavelength ($2\pi/k$)	2500 Å
Input laser power	30 MW
Dimensionless r.m.s. wiggler vector potential (a_w)	4.352
Wiggler length	30 m
Wiggler period ($2\pi/k_w$)	10 cm

FIGURE CAPTIONS

Figure 1. A three-dimensional plot of laser intensity vs. r and z inside the wiggler.

Figure 2. A cross-section of the laser intensity, with a least-squares Gaussian fit, at z = 10 m, in the exponential gain regime. The 1/e point of the electric field for the Gaussian fit (the light beam radius) is at 0.024 cm .

Figure 3. A cross-section of the laser intensity, with a least-squares Gaussian fit, at z = 25 m, after saturation. The light beam radius is 0.023 cm.

Figure 4. A cross-section of the laser intensity, with a least-squares Gaussian fit, at z = 30 m, the end of the wiggler. The light beam radius is 0.024 cm.

Figure 5. A cross-section of the phase ϕ of the complex electric field amplitude at the end of the wiggler, z = 30 m, with a least-squares parabolic fit. The decrease of ϕ with increasing r indicates that the light is <u>focusing</u> at the end of the wiggler.

8559v/0196v

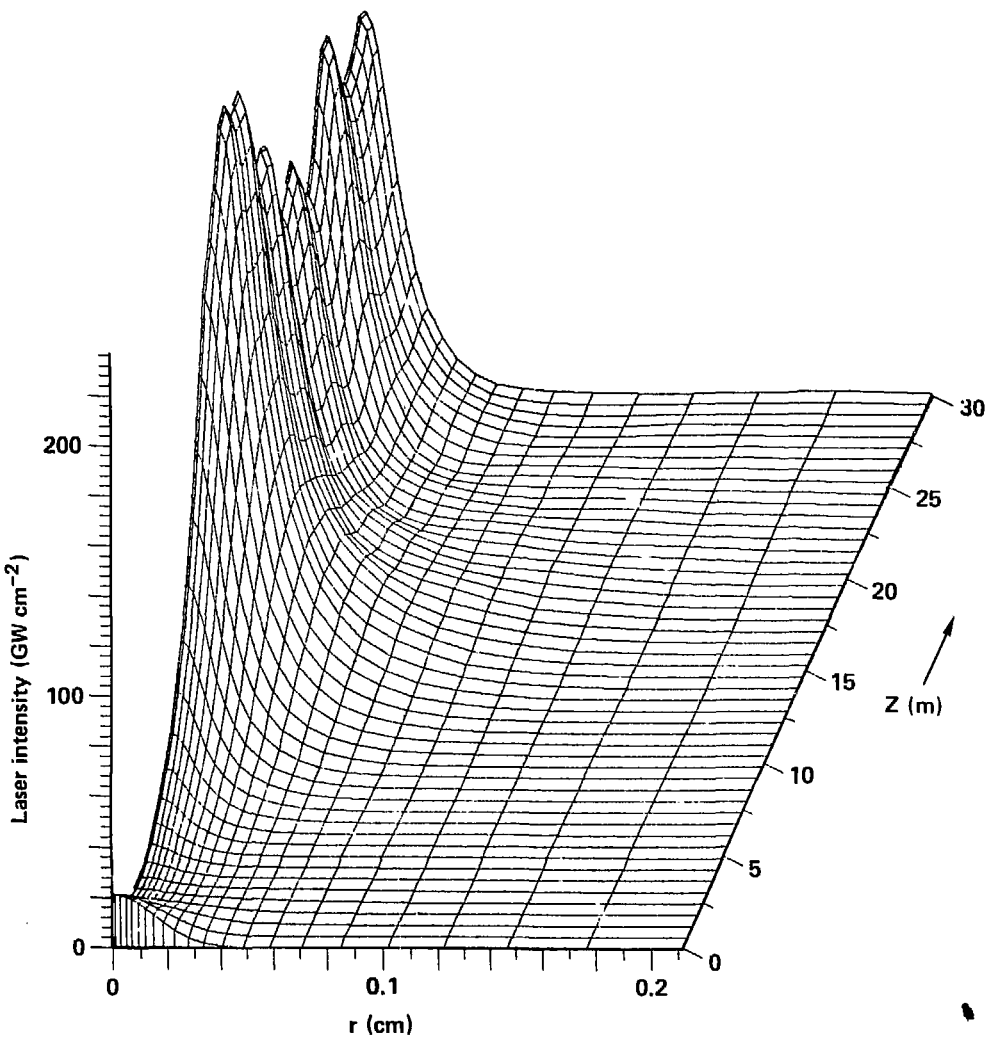

Figure 1

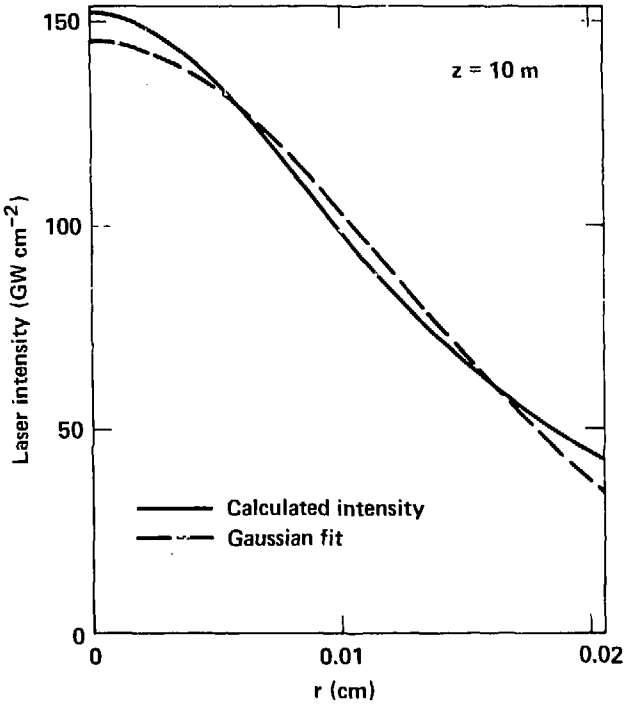
150
100
50
0
z = 10 m
Laser intensity (GW cm^{-2})
Calculated intensity
Gaussian fit
0
0.01
0.02
r (cm)

Figure 2

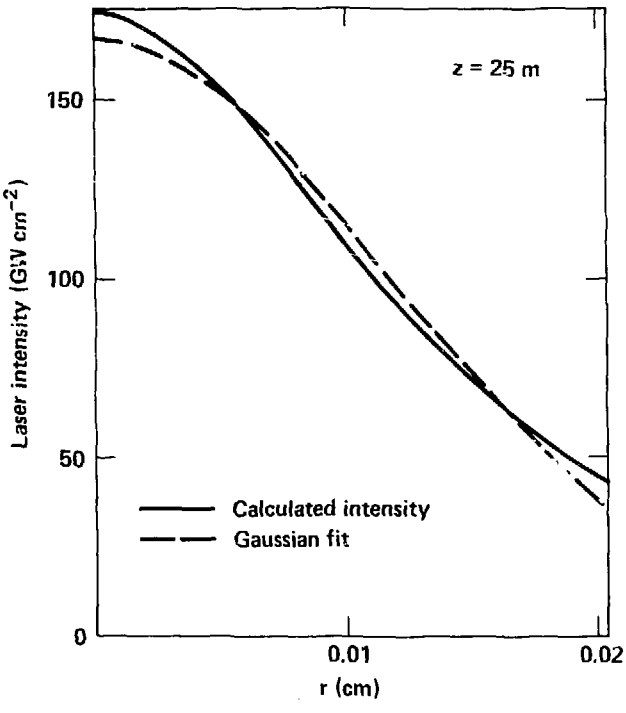
z = 25 m
150
100
50
0
Laser intensity (GW cm^{-2})
Calculated intensity
Gaussian fit
0.01
0.02
r (cm)

Figure 3

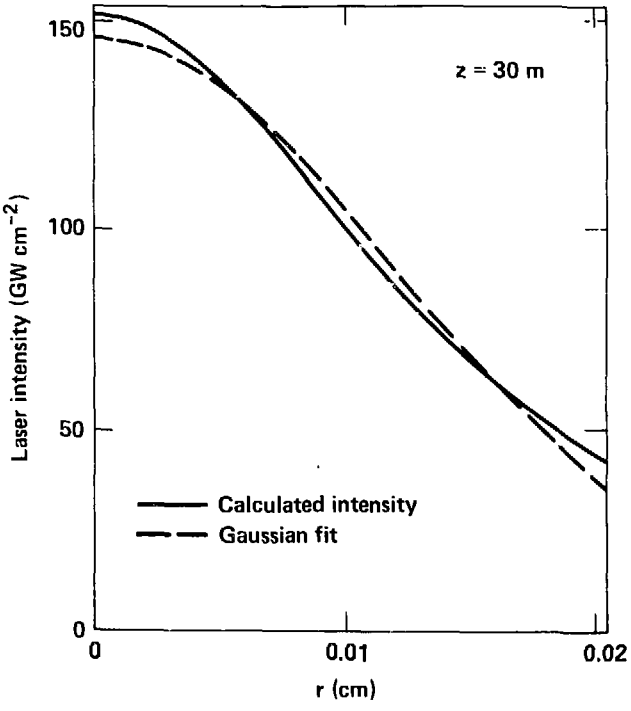
150
100
50
0
z = 30 m
Laser intensity (GW cm^{-2})
Calculated intensity
Gaussian fit
0
0.01
0.02
r (cm)

Figure 4

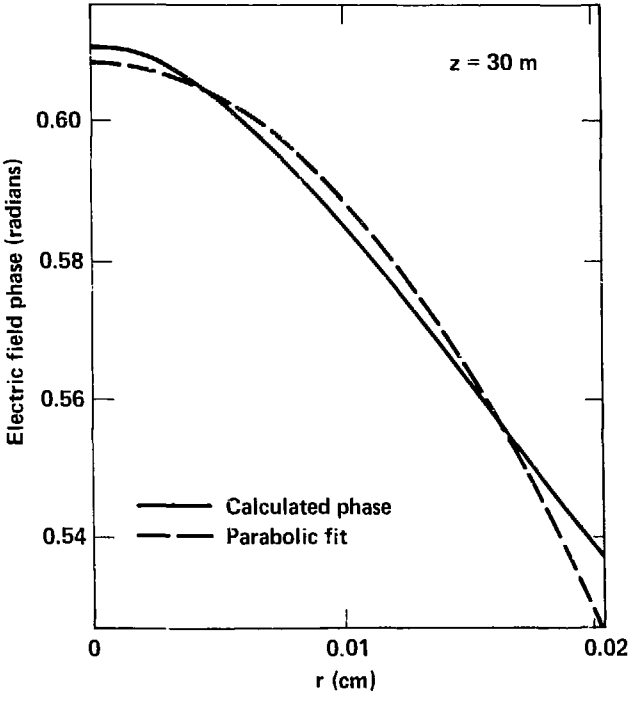
z = 30 m
0.60
0.58
0.56
0.54
Electric field phase (radians)
Calculated phase
Parabolic fit
0
0.01
0.02
r (cm)

Figure 5